ELSEVIER

Journal of Photochemistry and Photobiology A: Chemistry 122 (1999) 23–31

Journal of Photochemistry and Photobiology A:Chemistry

State of aggregation of bilirubin in aqueous solution: principal component analysis approach

Samir Kumar Patra, Anil Kumar Mandal, Medini Kanta Pal*

Department of Biochemistry and Biophysics, University of Kalyani, Kalyani 741235, West Bengal, India

Received 23 July 1998; received in revised form 17 November 1998; accepted 16 December 1998

Abstract

Principal component analysis (PCA) of the absorption spectra of the solutions of bilirubin with increasing its concentration at a fixed BSA concentration definitely shows that the pigment in aqueous solution remains as a mixture of tetramer and monomer in equilibrium. The association constant among the bilirubin molecules is as high as $\sim 10^4$. We have been able to resolve the observed spectra of aqueous bilirubin into component spectra absolutely characteristic of monomer and tetramer, showing peaks at 480 and 425 nm, respectively. The tetrameric form of bilirubin in solution fits well with the model of unit cell packing of four bilirubin molecules in solid crystalline powdered state. Hence, it has been speculated that bilirubin in solution persists as liquid crystal.

Keywords: Bilirubin; Aggregation; Kernicterus; Hepatic uptake; Liquid crystal

1. Introduction

The endobiotic substance bilirubin (BR), constantly produced in mammalian circulation due to break down of heme of hemoglobin of red blood corpuscles, is cytotoxic as well as neurotoxic pigment of jaundice [1–6]. The molecule is a substituted tetrapyrrole dicarboxylic acid consisting of two dipyrrole halves joined by a $-CH_2$ group [7–9]. The two halves are intramolecularly hydrogen bonded between each –COOH group of one half and the lactem (–NH–C=O) as well as the –NH groups of the other half; imposing folded, biplanar, ridge-tile, interconverting enantiomeric conformations [9–11]. Due to the presence of aromatic domains and imposed conformational restrictions for intramolecular hydrogen bonding, the molecule is sparingly soluble in water and extremely lipophilic in nature [6,10–14]. The lipophilic character of the pigment accounts for its deposition in the basal ganglia of brain cells (which are rich in phospholipids) of neonates having high bilirubin concentration, especially to those who have immatured blood brain barrier, causing bilirubin encephalopathy/kernicterus [4,13–16].

Though the science of bilirubin has been studying for over 60 years by different biochemical and biophysical technics, there is still much uncertainty regarding its solubility and modes of aggregation, which are crucially important for its hepatobiliary excretion, both in physiological and pathophysiological states. Earlier works opined that its folded biplanar structure no longer persists when bilirubin is in solution, and at moderate concentration bilirubin remains in dimer form which in turn self-associates to multimer when concentration is further increased [12,13,17–19]. However, recent report on bilirubin structure by heteronuclear overhauser effect NMR method [20], suggests the presence and persistence of folded intramolecularly hydrogen bonded conformers of bilirubin in solution.

In view of the above, the modes of aggregation of bilirubin in solution in the presence of bovine serum albumin (BSA) around physiological pH, and the effect of pigment concentration in this scenario have been thoroughly probed by us using absorption spectroscopy and applying principal component analysis (PCA) method [21–24].

2. Material and methods

2.1. Materials

Bilirubin IX-α (B4126), lot 57F-0111; BSA (A60003), lot 122H 9308 (essentially fatty acid free and prepared from

*Corresponding author. E-mail: mkpal@klyuniv.ernet.in

Abbreviations: BR, bilirubin; H_2BR, protonated bilirubin; Na_2BR, sodium bilirubinate; PCA, principal component analysis; BSA, bovine serum albumin

1010-6030/99/$ – see front matter
PII: S1010-6030(98)00465-1

fraction V) were purchased from Sigma Chemicals, USA. MOPS buffer was purchased from SRL, India. All other chemicals used were of AR/GR qualities.

As bilirubin is sparingly soluble in water and even in sodium bicarbonate solution unusual for a dicarboxylic acid [1,6,14,17,18], the solutions of bilirubin were prepared in aqueous NaOH medium considering its molecular weight of 584.6. Prior to each experiment 3.0 mg of the pigment was dissolved in 2.5 ml of 50.0 mM NaOH solution and volume made up to 50.0 ml with glass distilled water. Since, the pigment solution is light sensitive the container was wrapped with aluminium foil and placed in dark. The pH of the experimental solutions were adjusted by adding adequate amount of dilute HCl and then buffered at desired pH by 10.0 mM phosphate buffer, unless otherwise stated. Stock solution of BSA was prepared by dissolving it in 10.0 mM buffer solution (pH 7.5) and the strength of the solution was calculated according to the molecular weight 69 300 as described earlier [5,6,24].

The absorption spectra were recorded on a UV–Vis recording spectrophotometer, Shimadzu, model UV-160A, within 30 min of preparations of the experimental solutions.

2.2. Extended PCA method for equilibrium systems

This method has been described elsewhere [21] in detail, therefore, we describe here it in brief with some new idea. This is a very powerful method, not only for determining the number of coloured components in an equilibrium mixture, but also for determining their pure (individual) molar absorption coefficients ($\boldsymbol{\varepsilon}$) and equilibrium constant between either coloured or the coloured and colourless components, from an observed set of, say m, overlapping absorption spectra that can be obtained by varying the compositions between the components. From the m observed spectra a data matrix $\boldsymbol{d}$ of the order $(m \times n)$ can be constructed, whose element $d_{i,j}$ is the absorbance of the ith solution at the jth wavelength ($i = 1$ to m, $j = 1$ to n). Therefore, according to Beer's law for p-absorbing components in equilibrium ($p \leq m$),

$$\boldsymbol{d} = \boldsymbol{c} \times \boldsymbol{\varepsilon} \tag{1}$$

where $\boldsymbol{c}$ is the concentration matrix of the order $(m \times p)$, whose element $c_{i,j}$ is the equilibrium concentration of the jth component in the ith solution and $\boldsymbol{\varepsilon}$ is the pure molar absorption coefficient matrix of the order $(p \times n)$, whose element $\boldsymbol{\varepsilon}_{i,j}$ denotes molar absorption coefficient of the ith component at the jth wavelength. In most cases, $\boldsymbol{c}$ and $\boldsymbol{\varepsilon}$ are unknown; these quantities can be simultaneously determined by applying PCA method.

If the individual rows of $\boldsymbol{d}$ are divided by the respective initial or analytical concentration of any one of the p-absorbing species in m different mixtures, a new data matrix $\boldsymbol{\varepsilon}_a$, called apparent molar absorption coefficient matrix of the particular component, is obtained.

The diagonalisation [25] of the product $(\boldsymbol{\varepsilon}_a^T \times \boldsymbol{\varepsilon}_a)$ or $(\boldsymbol{d}^T \times \boldsymbol{d})$, where $\boldsymbol{\varepsilon}_a^T$ and $\boldsymbol{d}^T$ are the transpose matrices of $\boldsymbol{\varepsilon}_a$ and $\boldsymbol{d}$, respectively, yields n-eigenvalues $(\lambda_1,\lambda_2,\lambda_3,\cdots\cdots,\lambda_n)$ and n-eigenvectors. The number of absorbing components representing the observed spectra are correctly determined from the relative magnitudes of the eigenvalues. The following relation between eigenvalues holds for p-absorbing components:

$$\lambda_1 \geq \lambda_2 \geq \lambda_3 \geq \cdots\cdots \geq \lambda_p \gg \lambda_{p+1} \geq \cdots\cdots \geq \lambda_n > 0 \tag{2}$$

i.e., for p-absorbing components there appears a large gap between the pth and $(p + 1)$th eigenvalues. Thus, for p-absorbing components p-eigenvalues become significant, and hence the corresponding p-eigenvectors are considered as the fundamental spectra and common to the all m observed spectra. From the p-eigenvectors an eigenvector matrix $\boldsymbol{e}$ of the order $(p \times n)$ is then constructed. The matrices $\boldsymbol{\varepsilon}_a$ and $\boldsymbol{d}$ can now be expressed by the linear combinations of the p-eigenvectors as:

$$\boldsymbol{d} = \boldsymbol{f} \times \boldsymbol{e} \tag{3}$$

$$\boldsymbol{\varepsilon}_a = \boldsymbol{L} \times \boldsymbol{e} \tag{4}$$

where $\boldsymbol{f}$ and $\boldsymbol{L}$ are two linear combination coefficient matrices of the order $(m \times p)$. Since $\boldsymbol{d}$, $\boldsymbol{\varepsilon}_a$ and $\boldsymbol{e}$ are known, $\boldsymbol{f}$ and $\boldsymbol{L}$ can be calculated from the relations, $\boldsymbol{f} = \boldsymbol{d} \times \boldsymbol{e}^{-1}$ and $\boldsymbol{L} = \boldsymbol{\varepsilon}_a \times \boldsymbol{e}^{-1}$, provided $\boldsymbol{e}$ is a square matrix. But in most cases, $\boldsymbol{e}$ is not a square matrix; to solve this problem both sides of the Eqs. (3) and (4) are multiplied by $\boldsymbol{e}^T$, the transpose of $\boldsymbol{e}$ matrix, and then inverted as follows:

$$\boldsymbol{d} \times \boldsymbol{e}^T = \boldsymbol{f} \times (\boldsymbol{e} \times \boldsymbol{e}^T) = \boldsymbol{f} \times \boldsymbol{r} \tag{5}$$

where $\boldsymbol{r} = (\boldsymbol{e} \times \boldsymbol{e}^T)$, is a square matrix. Therefore, $\boldsymbol{f}$ and $\boldsymbol{L}$ become,

$$\boldsymbol{f} = (\boldsymbol{d} \times \boldsymbol{e}^T) \times \boldsymbol{r}^{-1} \tag{6}$$

and

$$\boldsymbol{L} = (\boldsymbol{\varepsilon}_a \times \boldsymbol{e}^T) \times \boldsymbol{r}^{-1} \tag{7}$$

The characteristic of the matrix $\boldsymbol{L}$ is that its row elements satisfy a common equation. For example, when $p = 2$, the plot of the elements in the first column of $\boldsymbol{L}$ against the corresponding elements in the second column, gives a straight line.

Like $\boldsymbol{d}$ and $\boldsymbol{\varepsilon}_a$, the pure molar absorption coefficient matrix $\boldsymbol{\varepsilon}$ of type $(p \times n)$ should also be related to the eigenvector matrix $\boldsymbol{e}$ by a transformation matrix $\boldsymbol{t}$ of the type $(p \times p)$ as:

$$\boldsymbol{\varepsilon} = \boldsymbol{t} \times \boldsymbol{e} \tag{8}$$

Therefore, from Eqs. (1), (3) and (8), we have,

$$\boldsymbol{c} = \boldsymbol{f} \times \boldsymbol{t}^{-1} \tag{9}$$

Now, only the matrix $\boldsymbol{t}$ is unknown, which has to be determined for determining $\boldsymbol{c}$ and $\boldsymbol{\varepsilon}$ matrices. It is to be

seen that the elements of different rows of the required matrix $\boldsymbol{t}$ must also satisfy the equation derived from $\boldsymbol{L}$ matrix; this is because, if any one of the rows of the matrix $\boldsymbol{\varepsilon}_a$ is a pure molar absorption spectrum of a particular component, the corresponding row of $\boldsymbol{L}$ must also be a row of the required matrix $\boldsymbol{t}$. With the help of a simple computer programming using loops, various reasonable $\boldsymbol{t}$ matrices satisfying the equation obtained from $\boldsymbol{L}$ matrix, can be constructed. Now, possible equilibrium schemes for the system under investigation is then assumed. For each $\boldsymbol{t}$ matrix, one would get $\boldsymbol{\varepsilon}$ and $\boldsymbol{c}$ matrices as well as m equilibrium constants corresponding to m experimental solutions, using any of the possible equilibrium schemes. If the system contains q components out of which p are absorbing ($p \leq q$), $(p - q)$ non-absorbing components are also needed for equation of mass balance, and their equilibrium concentrations can be calculated from their initial or analytical concentrations, and from the matrix $\boldsymbol{c}$. Only, for correct $\boldsymbol{t}$ matrix and proper equilibrium scheme, all the elements of $\boldsymbol{\varepsilon}$ and $\boldsymbol{c}$ would be positive as well as the m equilibrium constants would be the same or nearly the same. For the last criterion, another parameter S defined by,

$$S = \frac{\left\{ (1/m) \sum_{i=1}^{m} (k_i - K)^2 \right\}^{1/2}}{K} \tag{10}$$

can be used as a monitor, which would be zero or nearer to zero; K denotes the average value of the m equilibrium constants. For incorrect $\boldsymbol{t}$ matrices, or for improper equilibrium scheme, either S value does not minimise or some of the elements of $\boldsymbol{\varepsilon}$ or $\boldsymbol{c}$ become negative.

3. Results and discussion

It has already been mentioned that unconjugated bilirubin IX-α, when fully protonated, adopts a folded, biplanar, ridge-tile conformation (Fig. 1), stabilised by intramolecular hydrogen bonds [6–11]. These hydrogen bonds limit the interaction with water of all the polar groups in the molecule, accounting for the very low aqueous solubility of unconjugated bilirubin diacid [8,12,19,26–30].

Fig. 2 shows the absorption spectra of 7.60 μM BR IX-α in aqueous medium at four different pH. It is clear from Fig. 2 that in the pH range of 6.6–9.2 BR depicts a broad peak around 438 nm, our PCA result (follows) show that this broad peak is due to tetramer of BR. It was observed that at pH 6.6 an opalescence gradually appeared without any obvious precipitation and at all other pH above 7 the solutions were clear. The absorption spectrum of bilirubin was also measured at the same pH 6.6 but in the presence of 10 mM MOPS buffer. This was done by lowering the pH of the stock solution of BR (in aqueous NaOH medium) by adding adequate dilute HCl solution to pH 7.2, followed by pipetting a desire volume of this solution to the MOPS buffer (pH 6.6) so that the final bulk concentration of BR was 7.6 μM. The corresponding absorption spectrum (a′) overlaps with the spectrum (a). It is interesting to note that at

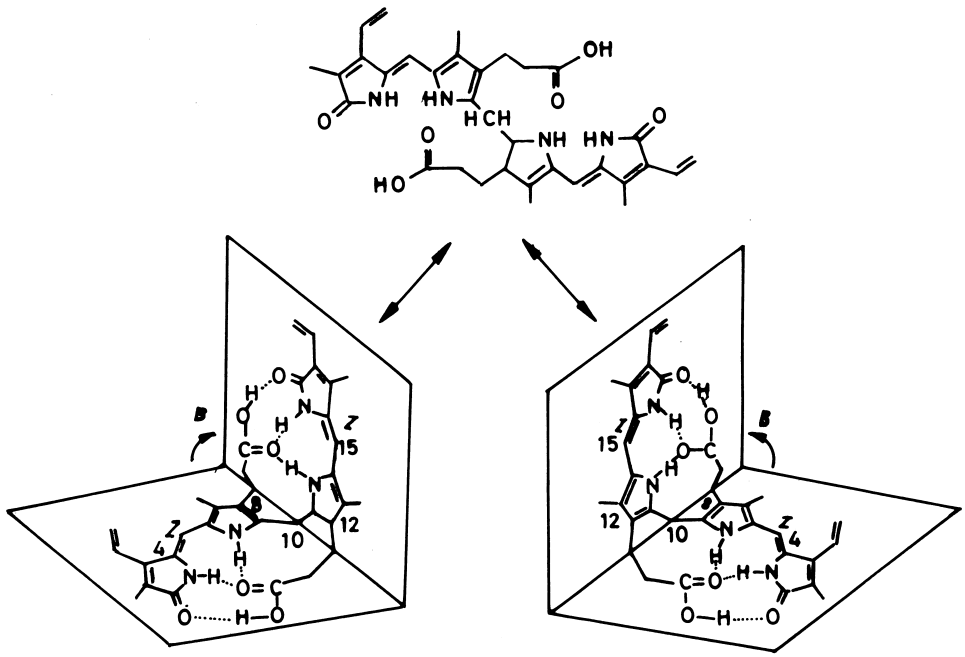

Fig. 1. The representation of the structure of the unconjugated bilirubin IX-α diacid. The upper conformation is a planar projection of the conformation adopted by rotation of the two dipyrrinones around the central (C_{10}) bridge, which permits the formation of internal bonds as shown in the lower enantiomeric conformations (for detail see Ref. [11–13]).

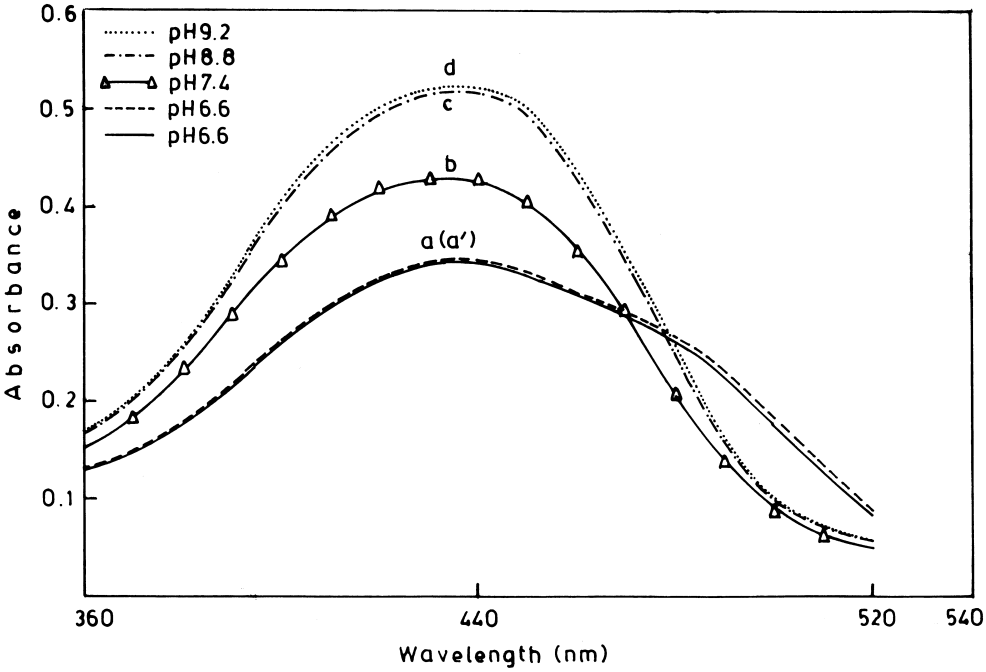

Fig. 2. Absorption spectra of 7.60 μM bilirubin at different pH.

acidic pH, whether buffered or not, BR shows a red-shifted shoulder around 480 nm, may be the λ_{max} of monomeric BR [6,24,31–33]. The appearance of the shoulder around 480 nm may be due to a partial hindrance of aggregation of protonated bilirubin (H_2BR).

It has to be pointed out, here, about the aqueous solubility of BR, otherwise one may raise question regarding the use of the concentrations of BR in our present work. Actually, there is a lot of controversy regarding aqueous solubility and dissociation constants of the bilirubin diacid. Near physiological or slightly alkaline pH the solubility of bilirubin has been found to vary extensively (10 nM to 15 mM) as shown by the experimental studies of crystal dissolution [13,14,34–37] or acidification of sodium bilirubinate (Na_2BR) [37–39]. On the other hand, Ostrow and co-workers [17] determined the aqueous solubility and pK_a values of H_2BR by using a complicated solvent partition technique, and they concluded that the maximum aqueous solubility of H_2BR is about 66 nM and the pK_a values are not much different, but are similar with the values $pK_{a1} = 8.12$ and $pK_{a2} = 8.44$. The partition data [17] show that the total solubility of BR increases with increasing pH; it is 80 nM at pH 6.8 and 170 nM at pH 8.0; and above pH 8.0, where the –COOH groups are ionised, the solubility rises steeply and it becomes 1 mM at pH 9.0 and 60 mM at pH 9.5. Recently, Lightner et al. [40] determined the pK_a values of ^{13}C-enriched (^{13}COOH) mesobilirubin XII-α, the corresponding biliverdin and several monopropionic model compounds by ^{13}C NMR spectroscopy, and suggested that the pK_a values of bilirubin would be around 4.2 and 4.9. They indicated [40] that intramolecular hydrogen bonding has no effect on the acid dissociation of bilirubin, contrary to the interpretation for high pK_a values of BR from partition method [17]. Thus, it appears that there is still much controversy regarding the solubilities and pK_a values of BR.

The series of spectra in Fig. 3 show the effect of increasing BSA on 16.0 μM aqueous BR at pH 7.8 ± 0.2. The spectrum 1 of BR alone shows a broad peak around 438 nm; on addition of BSA the absorbance at 438 nm progressively decreases with congruent rise in the absorbance at longer wavelength and eventually a relatively sharp peak appears at 476 ± 2 nm. The optimum concentration of BSA capable of inducing this red shifted peak is 32.0 μM (spectrum 14); still higher concentration of BSA does not have any further effect. All the spectra 1–16 pass through a clear isosbestic point at 445 nm, strongly indicating an equilibrium existence of two absorbing species [18]. We utilised the data from this set of spectra to calculate the association constant(s), K_a of BSA–BR using the Scatchard relation [41],

$$\frac{r}{c} = K_a \times n - K_a \times r \tag{11}$$

where r, c, K_a and n are the fraction of ligand bound to the polymer, free ligand concentration, association constant of the ligand and number of binding sites per polymer molecule, respectively [5,24,42]. The inset of the same Fig. 3 shows the corresponding Scatchard plot. The plot shows two slopes indicating two different affinity sites per BSA molecule for BR. The line with lower slope covers the region at low BSA concentration, where the ligand will be constrained to bind at low affinity site; obviously, the steeper line is relevant to the binding of BR at the high affinity site in the presence of excess BSA. The association constant values for binding at the high and low affinity sites, calculated from the

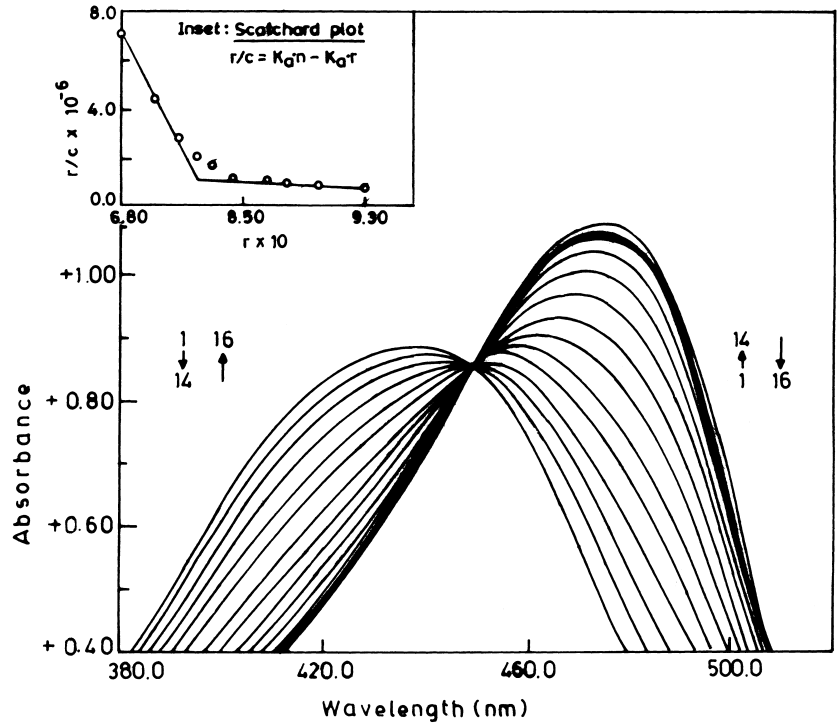

Fig. 3. Spectra 1 to 16 are absorption spectra of 16.0 μM bilirubin in the presence of 0.0, 2.0, 4.0, 6.0, 8.0, 10.0, 12.0, 14.0, 16.0, 18.0, 20.0, 22.0, 24.0, 32.0, 40.0 and 72.0 μM BSA, respectively, buffered at pH 7.8 at 23 ± 1°C. Inset: the corresponding Scatchard plot.

respective slopes, come to be 7.30×10^6 and $4.50 \times 10^5\ M^{-1}$, respectively, which are in reasonable agreement with the literature values [5,24,31,32]. It is apparent from the Scatchard relation that the intercept of the plot of *r*/*c* versus *r* gives the number (*n*) of ligand (BR) bound per BSA molecule; for our data the values of *n* are 1.0 and 0.70 for high and low affinity sites, respectively. Since there are two well defined affinity sites for bilirubin per albumin molecule and, one and only one bilirubin binds per site, one can rationally infer that bound bilirubin molecules will be in the monomeric form at least up to bilirubin/albumin ratio not exceeding 1.0.

Bilirubin IX-α in aqueous solution can self-associate in a manner reminiscent to that of many water soluble dyes, certain steroid amphiphiles and porphyrins; and dimers are formed in dilute solution and these in turn self-associate to form multimers as the concentration is increased [14,18,24]. This interpretation of dimerisation and eventual multimerisation of BR in aqueous solution on increasing concentration has been analogically inferred from the observed spectral changes. The interesting results of the application of PCA method [21,22] to the concentration dependent spectra of BR are presented here. The method leads to a definite conclusion regarding the state of aggregation of aqueous BR without any ambiguity and the complete resolution of the observed experimental spectra into the pure component spectra of the monomeric and aggregated forms of BR as well as the accurate calculation of the equilibrium constant between monomer and aggregates. This is the first mathematical approach to resolve the absorption spectra of bilirubin in solutions by applying PCA method. Our interesting results will show that BR exists only in the form of two absorbing species, namely monomer and tetramer, at least up to 36.65 μM around pH 7.6 in the presence of a limited concentration of BSA. The monomeric BR exhibits a relatively sharp peak at 480 nm and the tetramer shows a broad peak centered at 425 nm. The observed experimental spectra of BR represent the combination of the absorption spectra of these two species, in relative amounts, depending on total BR concentration.

The spectral changes of BR on varying its concentration from 16.42 to 36.65 μM at pH 7.6 ± 0.2 at a fixed concentration (16.2 μM) of BSA (spectra (a)–(f)) are shown in Fig. 4. In view of the very limited solubility of BR in aqueous solution, a fixed concentration of BSA was added to increase the solubility of BR to give stable solutions over a wider range of concentration. It has been observed that a solution of bilirubin around neutral pH on standing overnight results in a marked reduction in absorbance, but in the presence of BSA does not show any change in the absorbance indicating the solution of BR stable. The apparent molar absorption (ε_a) spectra corresponding to the spectra of Fig. 4 are shown in Fig. 5; the clear isosbestic point at 445 nm indicates an equilibrium co-existence of two absorbing species [18]. One of these is of course monomeric bilirubin showing λ_{max} at 480 nm [6,24,31–33]. A data matrix ***d*** of the order (47 × 6) was constructed from the spectra (a)–(f) of Fig. 4, taking the absorbance data at 3 nm

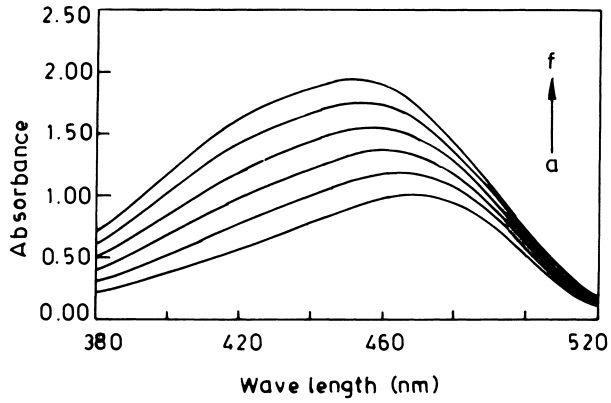

Fig. 4. Spectra (a) to (f) are absorption spectra of 16.42, 20.52, 24.63, 28.73, 32.84 and 36.65 μM BR, respectively, in presence of a fixed concentration of 16.2 μM BSA, buffered at pH 7.6 at 23 ± 1°C.

intervals from 382 to 520 nm. The diagonalisation [25] of the product of the data matrix $\boldsymbol{d}$ and its transpose $\boldsymbol{d}^{\mathrm{T}}$ results in 47 eigenvalues and corresponding 47 eigenvectors. Among the 47 eigenvalues only two are significant, viz. 321.4625 and 1.8330, and others are <0.0002 indicating that all the test solutions of the spectra (a)–(f) of Figs. 4 and 5 contain two and only two absorbing species. The eigenvectors corresponding to the two significant eigenvalues, shown in Fig. 6, are the fundamental spectra to all the observed spectra (a)–(f). Therefore, the data matrix $\boldsymbol{d}$ and the apparent molar absorption coefficient matrix ε_{a}, constructed from the spectra (a)–(f) of Fig. 5, can be expressed by the relations, $\boldsymbol{d} = \boldsymbol{f} \times \boldsymbol{e}$ and $\varepsilon_{\mathrm{a}} = \boldsymbol{L} \times \boldsymbol{e}$, where $\boldsymbol{f}$ and $\boldsymbol{L}$ are linear combination coefficient matrices of the order (6 × 2). The significance of the matrix $\boldsymbol{L}$ has already been mentioned in Section 2. The plot of L_{i1} versus L_{i2} gives, as expected, a straight line (inset of Fig. 6) having slope = 4.85 and intercept = -1.2901×10^6. The molar absorption coefficient matrix $\boldsymbol{\varepsilon}$ (Eq. (1)) of the pure components is also related to the eigenvector matrix $\boldsymbol{e}$ by a transformation matrix $\boldsymbol{t}$ of the order (2 × 2) as $\boldsymbol{\varepsilon} = \boldsymbol{t} \times \boldsymbol{e}$. To determine $\boldsymbol{\varepsilon}$ and $\boldsymbol{c}$ matrices one has to determine the transformation matrix $\boldsymbol{t}$. The elements of the matrix $\boldsymbol{t}$ also satisfy the equation obtained from the matrix $\boldsymbol{L}$, that is, the elements of $\boldsymbol{t}$ would also lie on the line of the inset of Fig. 6. The correct elements of the matrix $\boldsymbol{t}$ can be obtained by considering an appropriate equilibrium scheme for the system as mentioned earlier (PCA method). We consider here the equilibrium scheme as,

$$n\,\mathrm{BR} \rightleftharpoons (\mathrm{BR})_n$$

where $n = 1,2,3,4,\ldots$, etc. It is apparent from the analysed data summarised in Table 1 that only for $n = 4$ and for the elements of $\boldsymbol{t}$ corresponding to the points X and Y on the line of the inset of Fig. 6, the variation of coefficient S (Eq. (10)) becomes minimum (0.0252) as well as all the elements of $\boldsymbol{\varepsilon}$ and $\boldsymbol{c}$ matrices become non-negative and reasonable. For values of n from 1 to 3, the S values are low, but $\boldsymbol{\varepsilon}$ values come out to be negative in the lower and/or higher wavelength regions, and hence not acceptable. The values 5 and 6 (and also higher than 6) for n are also rejected because the

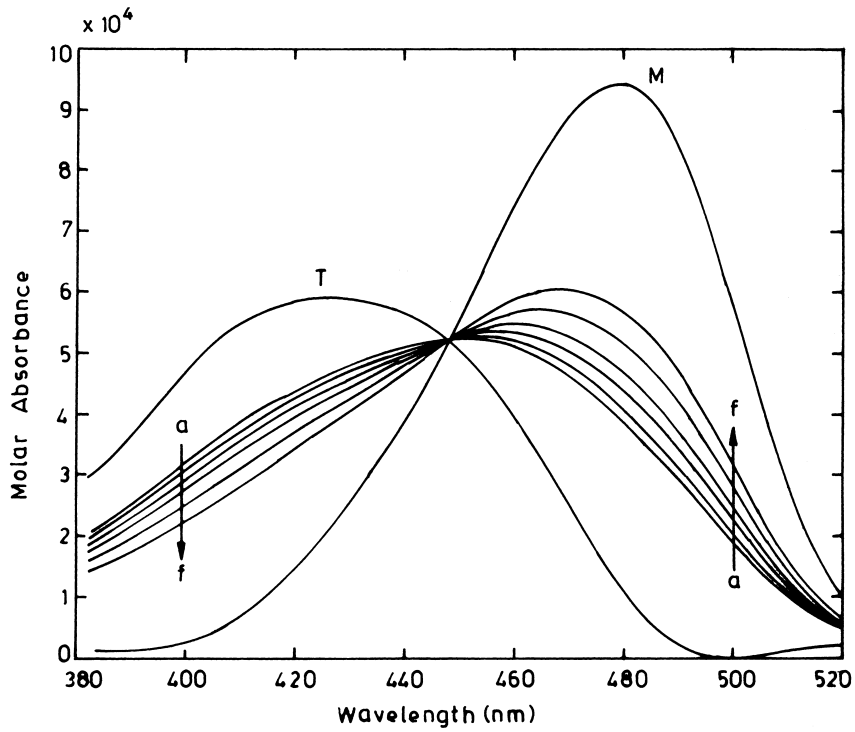

Fig. 5. Spectra (a) to (f) are the apparent molar absorption (ε) spectra corresponding to the spectra of Fig. 4 and the spectra (M) and (T) are the resolved molar absorption spectra of the pure monomer and tetramer species of BR.

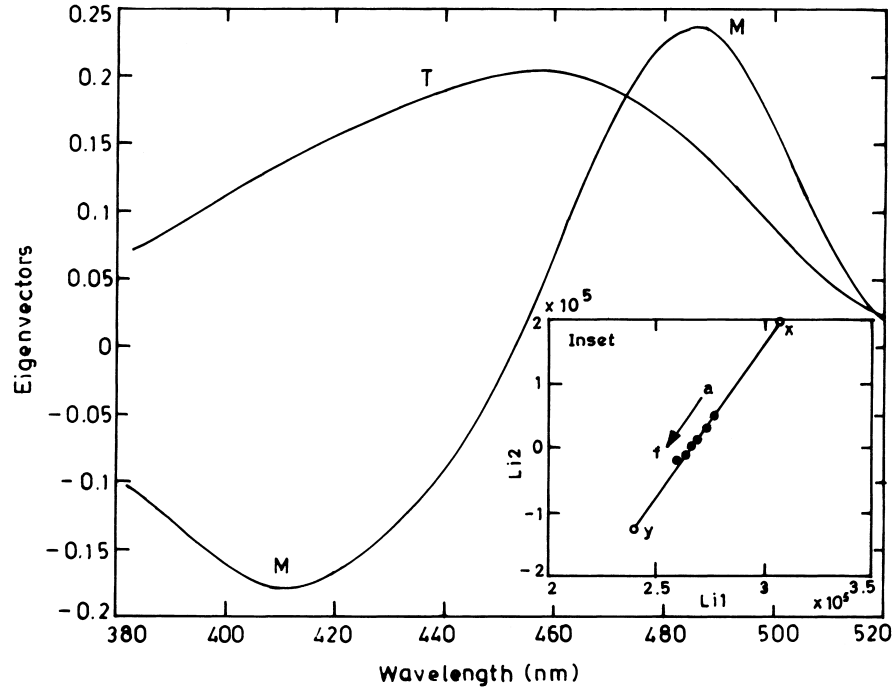

Fig. 6. T and M are eigenvectors corresponding to the significant eigenvalues of 321.4625 and 1.8330, respectively. Inset: the plot of L_{i1} vs. L_{i2} of the linear combination coefficient matrix $\boldsymbol{L}$.

Table 1
Data of PCA of absorption spectra

n	S	Lower wavelength region and ε values for monomer	Higher wavelength region and ε values for aggregate
1	0.0474	382–440 nm where ε values are −ve, min. $\varepsilon = -12.13 \times 10^4$ at 409 nm.	457–520 nm where ε values are −ve, min. $\varepsilon = -22.60 \times 10^4$ at 487 nm.
2	0.0369	382–421 nm where ε values are −ve, min. $\varepsilon = -1.80 \times 10^4$ at 403 nm.	471–518 nm where ε values are −ve, min. $\varepsilon = -2.22 \times 10^4$ at 487 nm.
3	0.0277	Same as to the spectrum M in Fig. 5.	480–514 nm where ε values are −ve, min. $\varepsilon = -1.03 \times 10^4$ at 493 nm.
4	0.0252	Same as to the spectrum M in Fig. 5.	Same as to the spectrum T in Fig. 5.
5	0.0524	In the lower region ε values are unreasonably high e.g., in the region 382–400 nm ε value varies from 0.8–1.2 × 10^4.	Same as to the spectrum T in Fig. 5.
6	0.0853	In the lower region ε values are unreasonably high e.g., in the region 382–400 nm ε value varies from 1.2–1.8 × 10^4.	Same as to the spectrum T in Fig. 5.

Note: ε values of the monomer and aggregates are positive at all wavelengths except indicated in the table.

contribution of the monomeric BR to the absorption spectra in the lower wavelength region though positive is unreasonably high as well as the S values are higher compared to that for $n = 4$. Since the equilibrium is in between two absorbing species, monomer and tetramer, the expected low contributions of the monomer and tetramer, respectively at the lower and higher wavelength regions of the absorption spectra are also fulfilled [43], as is apparent from the resolved molar absorption coefficient spectra of the monomer (M) and tetramer (T) shown in Fig. 5. The striking similarity between the spectra 14 to 16 of Fig. 3 and the resolved spectrum M (Fig. 5) is to be noticed. The monomeric spectrum (M) exhibits peak at 480 nm and that of tetramer (T) shows a broad peak centered at 425 nm. Patra and Pal's [6] recent report shows that bilirubin in the presence of BSA exhibits bisignate CD spectra; Lightner and his co-workers [11] have shown that bisignate CD spectra of BR result in due to ridge-tile conformation of BR. Thus, BR in the presence of BSA retains its ridge-tile conformation. The tetramer of BR show a blue-shifted peak at 425 nm compared to the monomeric peak at 480 nm; it has been established that the blue shifted peak results from the stacking of the planar chromophoric molecules [44,45]. Thus, the exhibition of blue shifted peak at 425 mm by BR is of course due to stacking of four BR molecules through planar halves of each ridge-tile interleaved with a similar but inverted stack as in unit cell packing of bilirubin molecules shown by Bonnett et al. [46]. Therefore, from PCA results it

Table 2
Results of PCA analysis of BR solutions at 23 ± 1°C

Spectra	[BR] (total) (μM)	[Monomer] (μM)	[Tetramer] in monomeric unit (μM)	$K \times 10^{-14}$
(a)	16.42	9.07	7.35	2.7374
(b)	20.52	10.02	10.50	2.5934
(c)	24.63	10.65	13.98	2.6882
(d)	28.73	11.38	17.35	2.5932
(e)	32.84	11.77	21.07	2.7431
(f)	36.65	12.21	24.44	2.7514

Note: average value of the equilibrium constants (K) = 2.684×10^{-14}.

can rationally be concluded that BR in solution, at least up to the concentration of 36.65 μM at pH 7.6 ± 0.2 in presence of 16.2 μM BSA, exists in two forms, namely monomer and tetramer in equilibrium. The average equilibrium constant (K), thus obtained from PCA result, comes to be 2.6844×10^{14}. The total, monomer and tetramer concentrations of BR and the values of K for the respective solutions of the spectra of Fig. 4 are shown in Table 2. It is to be mentioned that as the S value for monomer/tetramer equilibrium is sufficiently low (0.0252), the non-absorbing components have not been considered in the equilibrium scheme.

It is evident from the spectra shown in Figs. 3–5 that the tetramer species of BR predominates in aqueous solution, and the $4BR \rightleftharpoons BR_4$ equilibrium progressively shifts to the monomeric form with increasing albumin concentration. This shift in equilibrium is practically completed with two-fold excess of protein. With these results, and the report of Nogles and Lightner [20] that BR IX-α in aqueous solution persists in its folded, biplanar, ridge-tile conformation (Fig. 1); we propose that BR IX-α in solution may exist as liquid crystal. If so, the tetrameric aggregate fits well with the unit cell packing model of Bonnett et al. [46] for crystalline powdered state. Our observation also suggests that in physiological conditions hepatocellular uptake of bilirubin may be possible by diffusion controlled mechanism [47–49] prior to formation of aggregates. But in case of hyper bilirubinemia aggregation will happen before hepatic uptake causing accumulation of the pigment in the blood and hence, unusual diffusion of the pigment to the tissues and cells all throughout the body.

References

[1] C. Tiribelli, J.D. Ostrow, Hepatology 24 (1996) 1296–1311.
[2] J.D. Ostrow, in: J.D. Ostrow (Ed.), Bile Pigments and Jaundice; Molecular, Metabolic and Medical Aspects, Marcel Dekker, New York, 1986, pp. 1–6.
[3] D. Bartlid, New York State Med. J. 91 (1991) 489–492.
[4] T.W.R. Hansen, Clin. Pediatr. (Phila, USA) 38 (1994) 452–459.
[5] S.K. Patra, M.K. Pal, J.M.S. – Pure Appl. Chem. A 34(9) (1997) 1569–1579.
[6] S.K. Patra, M.K. Pal, Eur. J. Biochem. 246 (1997) 658–664.
[7] G. LeBas, A. Allegret, Y. Mauguen, G.M. Sheldrick, C. de Rango, M. Bailly, Acta Crystallogr. B36 (1980) 3007–3111.
[8] H. Falk, in: J.D. Ostrow (Ed.), Bile Pigments and Jaundice; Molecular, Metabolic and Medical Aspects, Marcel Dekker, New York, 1986, pp. 7–29.
[9] R. Bonnett, J.E. Davies, M.B. Hursthouse, G.M. Sheldrick, Proc. R. Soc. London B 202 (1978) 249–268.
[10] G. Blauer, G. Wagniere, J. Am. Chem. Soc. 97 (1975) 1949–1954.
[11] R.V. Person, B.R. Peterson, D.A. Lightner, J. Am. Chem. Soc. 116 (1994) 42–59.
[12] C. Tiribelli, J.D. Ostrow, Hepatology 17 (1993) 715–736.
[13] J.D. Ostrow, P. Mukerjee, C. Tiribelli, J. Lipid Res. 35 (1994) 715–737.
[14] R. Brodersen, J. Biol. Chem. 254 (1979) 2364–2369.
[15] D. Bartlid, Clin. Perinatol. 17 (1990) 449–465.
[16] R. Brodersen, L. Stern, Acta Paediatr. Scand. 79 (1990) 12–19.
[17] J-S. Ham, J.D. Ostrow, P. Mukerjee, L. Celic, J. Lipid Res. 33 (1992) 1123–1137.
[18] M.C. Carey, A.P. Koretsky, Biochem. J. 179 (1979) 675–689.
[19] D. Kaplan, G. Navon, J. Chem. Soc., Perkin Trans. II (1981) 1374–1383.
[20] D. Nogles, D.A. Lightner, J. Biol. Chem. 270 (1995) 73–77.
[21] M. Takatsuki, K. Yamaoka, J. Sci. Hirosima Univ. Ser. A 40 (1976) 387–415.
[22] K. Yamaoka, M. Takatsuki, Bull. Chem. Soc. Jpn. 51 (1978) 3182–3192.
[23] A.K. Mandal, M.K. Pal, J. Colloid Interface Sci. 192 (1997) 83–93.
[24] S.K. Patra, Ph.D. Thesis, University of Kalyani, Kalyani, West Bengal, India, 1996.
[25] Matlab, The Math Works Inc., 20 North Main St., Suite 250, Sherborn, MA 017770 (617) 653–1415.
[26] D.A. Lightner, R.V. Person, B.R. Peterson, G. Puzicha, Y.M. Pu, S.E. Boiadjiev, in: R.R. Brige, L.A. Nafie (Eds.), Biomolecular Spectroscopy II, Soc. Photo-Optical Instrument. Engin., Bellingham, WA, 1991, pp. 1–13.
[27] A.F. McDonagh, D.A. Lightner, in: K.W. Bock, W. Gerok, S. Matern, R. Schmid (Eds.), Hepatic Metabolism and Disposition of Endo- and Xenobiotics, Kluwer Academic Publishers, Dodrecht, 1991, pp. 47–59.
[28] S.E. Boiadjiev, R.V. Person, G. Puzicha, C. Knobler, E. Maverick, K.N. Trueblood, D.A. Lightner, J. Am. Chem. Soc. 114 (1992) 10123–10133.
[29] Y.Z. Hsieh, M.D. Morris, J. Am. Chem. Soc. 110 (1988) 62–67.
[30] B. Yang, R.C. Taylor, M.D. Morris, X.Z. Wang, J.G. Wu, B.Z. Yu, G.X. Xu, Spectrochim. Acta 49A (1993) 1735–1749.
[31] R.F. Chen, in: A.A. Thaer, M. Sernetz (Eds.), Fluorescence Technique in Cell Biology, Springer, Heidelberg, 1973, pp. 273–282.
[32] S. Tayyab, M. Abul Quasim, Biochem. Int. 18 (1989) 343–349.
[33] R.G. Reed, J. Biol. Chem. 252 (1977) 7483–7487.
[34] J.T.G. Overbeek, C.L.J. Vink, H. Deenstra, Rec. Trav. Chim. Pays-Bas 74 (1955) 81–84.
[35] Y. Moroi, R. Matura, T. Hisadome, Bull. Chem. Soc. Jpn. 58 (1985) 1426–1431.

[36] R. Brodersen, in: J.D. Ostrow (Ed.), Bile Pigments and Jaundice; Molecular, Metabolic and Medical Aspects, Marcel Dekker, New York, 1986, pp. 157–181.
[37] J.D. Ostrow, L. Celic, P. Mukerjee, J. Lipid Res. 29 (1988) 335–348.
[38] U. Wosiewitz, U. Leuschner, Naturwiss 77 (1990) 232–234.
[39] T. Nakama, Fukuoka Acta Med. 67 (1976) 413–441.
[40] D.A. Lightner, D.L. Holmes, A.F. MaDonagh, J. Biol. Chem. 271 (1996) 2397–2405.
[41] G. Scatchard, J.S. Coleman, A.L. Shen, J. Am. Chem. Soc. 79 (1957) 12–21.
[42] M.K. Pal, J.K. Ghosh, Spectrochim. Acta 51A (1995) 489–498.
[43] Y.-P. Sun, D.F. Sears Jr, J. Saltiel, F.B. Mallory, C.W. Mallory, C.A. Buser, J. Am. Chem. Soc. 110 (1988) 6974.
[44] M.K. Pal, M. Schubert, J. Phys. Chem. 67 (1963) 1821.
[45] M.K. Pal, M. Schubert, J. Am. Chem. Soc. 84 (1962) 4384.
[46] R. Bonnett, J.E. Davies, M.B. Hursthouse, Nature 262 (1976) 326–328.
[47] S.D. Zucker, W. Goessling, M.L. Zeidel, J.L. Gollan, J. Biol. Chem. 269 (1994) 19262–19270.
[48] S.D. Zucker, J. Storch, M.L. Zeidel, J.L. Gollan, Biochemistry 31 (1992) 3184–3192.
[49] S.D. Zucker, W. Goessling, J.L. Gollan, J. Biol. Chem. 270 (1995) 1074–1081.